



XRD, DSC, and Dielectric Studies of MWNT-Doped Polymer Electrolytes for Supercapacitor Application

Neelesh Rai¹ · C. P. Singh¹ · Lovely Ranjta¹ · M. Z. A. Yahya²

Received: 4 September 2022 / Accepted: 28 December 2022 / Published online: 19 January 2023
© The Minerals, Metals & Materials Society 2023

Abstract

Recently, high ionic conducting composite polymer electrolytes have become of great interest on account of their probable applications in various electrochemical devices, such as batteries, supercapacitors, fuel cells, solar cells, etc. The aim of the present work is to cast a stable free-standing membrane of polyvinyl alcohol (PVA)-based nanocomposite polymer electrolyte (NCPE) gel membranes using ammonium acetate salt ($\text{NH}_4\text{CH}_3\text{COO}$) and multiwall carbon nanotube (MWNT) contents for supercapacitor applications. X-ray diffraction (XRD) studies revealed improvements in the amorphous nature. The average crystal size of the MWNT-doped NCPE system was found to lie in the range of 30–70 nm. The degree of crystallinity (χ_c) in this case shows a decrease of up to 35 wt.% with the increase in filler concentrations. The differential scanning calorimetry (DSC) studies show better thermal response upon the addition of MWNTs. Thermo-gravimetric analysis (TGA) studies reveal that the mass of nanocomposite polymer electrolyte gel decreases continuously with the increase in the MWNT contents. Dielectric loss studies have also been used to understand the conduction process in the system. The presence of α -relaxation was evidenced during loss measurements. The source of polarizability decreases with an increase of frequency, and finally disappears due to the inertia of mobile ions. Optimum conductivity was achieved at $5.49 \times 10^{-4} \text{ Scm}^{-1}$ for 1 wt.% MWCNT-embedded NCPE gel membranes. The electrical conductivity response seems to follow the universal power law. The studies suggest the development of environmentally friendly H^+ ion (proton) conducting-based supercapacitor applications.

Keywords XRD · DSC · TGA · dielectric loss · nanocomposite polymer gel electrolyte · supercapacitor

Introduction

Recently, gel polymer electrolytes (GPEs) have become known as promising applicants for various electrochemical devices, i.e., fuel cells, smart windows, supercapacitors, high-performance batteries, sensors, etc., on account of the possibility of achieving high electrical conductivity, better mechanical and thermal stability, and the capability to form suitable electrode–electrolyte contacts.^{1–4}

However, GPEs are limited by their thermal stability and poor mechanical properties, and by increased reactivity with ion–metal electrodes.^{5,6} In an effort to improve the above drawbacks, increasing the performance of GPEs by the addition of nanodimension organic/inorganic fillers has become an ever-increasing attractive approach, which will lead to enhanced ionic conductivity and improved mechanical and thermal stability and electrode–electrolyte interface stability by forming a filler network in the polymer matrix, inhibiting crystallization and reformation of polymer chains, which alter the crystallinity and stabilize the conductive amorphous phase.^{7–9}

Thus, a new class has emerged of nanocomposite polymer electrolyte (NCPE) gel membranes which are a better option that combine the liquid phase conductivity of GPEs and the improved mechanical properties.

Researchers in recent times have dispersed non-interacting filler particles, like SiO_2 , Al_2O_3 , TiO_2 , BiNiFeO_3 ferrite, etc., to overcome these drawbacks associated with the

✉ Neelesh Rai
neeshssi@gmail.com

¹ Department of Physics, AKS University, Satna, Madhya Pradesh 485001, India

² Faculty for Defense Science and Technology, Universiti Pertahanan Nasional Malaysia, 57000 Kuala Lumpur, Malaysia

GPEs.^{9–14} Owing to possibility of achieving maximal ionic conduction with protons or NH_4^+/H^+ ions as transporting species in gel electrolyte systems, they have been used in recent times as a host for the development of proton-conducting electrolytes.¹⁵ Among the different nanofillers used in the development of nanocomposite systems, multiwalled carbon nanotubes (MWNTs), which possess unique mechanical properties and good electrode–electrolyte contact, and are usually characterized by high thermal stability, have recently been suggested as effective active dispersoid material for the development of NCPE gel membranes.^{16,17} Looking into the favorable properties of MWNTs, an attempt has been made in the present work to improve the performance of polyvinyl alcohol (PVA)-based electrolyte membranes through the dispersal of MWNT fillers. Based on these considerations, we have attempted to develop a free-standing proton-conducting nanocomposite gel membrane dispersed by MWNTs, followed by its characterizations by x-ray diffraction (XRD), DSC, and TGA, dielectric measurements were carried out.

Materials and Methods

In the present investigation, PVA (average molecular weight: 124,000–186,000; Aldrich) was used; the hydrolysis degree of PVA is greater than 99%. Moreover, PVA is biodegradable and non-toxic as well as a solvent swollen type polymer. Ammonium acetate ($\text{NH}_4\text{CH}_3\text{COO}$) (AR grade sd fine) for developing a proton-conducting gel electrolyte and aprotic solvent dimethyl sulfoxide (DMSO) (Merck) were used for the synthesis of composite gel membranes. The MWNTs used in the study were obtained from Aldrich, with an average diameter 60–90 nm and length 3–5 μm . The PVA was dispersed in a solution of $\text{NH}_4\text{CH}_3\text{COO}$ in DMSO to form a pristine gel electrolyte (PVA- $\text{NH}_4\text{CH}_3\text{COO}$). Subsequently, composite polymer gel electrolyte viscous solutions were prepared by admixing the MWNTs in a pristine gel electrolyte solution in different weight proportions followed by thorough mixing at a slightly elevated temperature with a magnetic stirrer for 7–12 h. To obtain free-standing NCPE gel membranes, one portion of the solutions were poured into PC Petri dishes and covered with Al foil to avoid contamination. After synthesis, gels in the form of thin stable membranes were taken out.

The synthesized NCPE gel membranes have been distinguished with the help of different experimental probes to appraise their performance for device application. Structural morphology, complexation, and crystal size of different NCPE gel membranes were studied by an x-ray diffractometer (D2 Phaser 08 Discover; Bruker). Thermal behavior (DSC and TGA) of the NCPE system was carried out on a NETZSCH DSC model STA449F1 in the temperature range

of room temperature to 340°C at a heating rate of 3°C/min under an N_2 environment.

Dielectric parameters were extracted with the help of impedance data using the relationship:

$$\epsilon^* = \epsilon' - j\epsilon'' \quad (1)$$

where $\epsilon' = \frac{-Z''}{\omega C_0 (Z'^2 + Z''^2)}$ and $\epsilon'' = \frac{-Z'}{\omega C_0 (Z'^2 + Z''^2)}$ where, the angular frequency is $\omega = 2\pi f$, f is the frequency of the applied field, Z' is the real part, and Z'' the imaginary part of impedance and C_0 is the geometrical capacitance in vacuum of the same dimension as the sample films.

$[C_0 = \frac{0.0885A}{d} \text{ pF}]$, where A is the area of electrode and d is the thickness of the sample.

For dielectric relaxation studies of the many complex modules, M^* formalism is used. The real part, M' , and the imaginary part, M'' , of the complex modulus (M^*) can be evaluated from the impedance data:

$$M^* = M' + jM'' = \frac{1}{\epsilon^*} = j\omega\epsilon_0 Z'' \quad (2)$$

$$\text{where } M' = \frac{\epsilon'}{(\epsilon'^2 + \epsilon''^2)} \quad M'' = \frac{\epsilon''}{(\epsilon'^2 + \epsilon''^2)} \quad (3)$$

The tangent loss ($\tan\delta$) can be evaluated using relationship:

$$\tan\delta = \frac{\epsilon''}{\epsilon'} = \frac{Z''}{Z'} \quad (4)$$

Electrical conductivity measurements were performed in the frequency range varying from 1 to $10\text{E}+6$ Hz at various temperatures ranging between 25°C and 90°C, and have been calculated using the relationship:

$$\sigma_{ac} = \epsilon_0 \omega \epsilon_r \tan\delta \quad (5)$$

where ϵ_r (relative permittivity) = C/C_0 , ϵ_0 is the permittivity of the free space, $\omega = 2\pi f$, and f is the frequency of the applied field.

Results and Discussion

XRD Studies

The XRD patterns of the polymer gel electrolyte membranes of $\text{NH}_4\text{CH}_3\text{COO}:\text{PVA}$ without and with MWNT nanofillers along with pristine materials are shown in Fig. 1a–d. The XRD pattern of pure MWNT is shown in Fig. 1 (inset). The pattern displayed an intense diffraction peak around $2\theta = 26^\circ$, and low intense diffraction peaks around 44° , 53° , and 78° , which are assigned to (002), (100), (004), and (110) diffraction patterns of typical graphite, respectively.

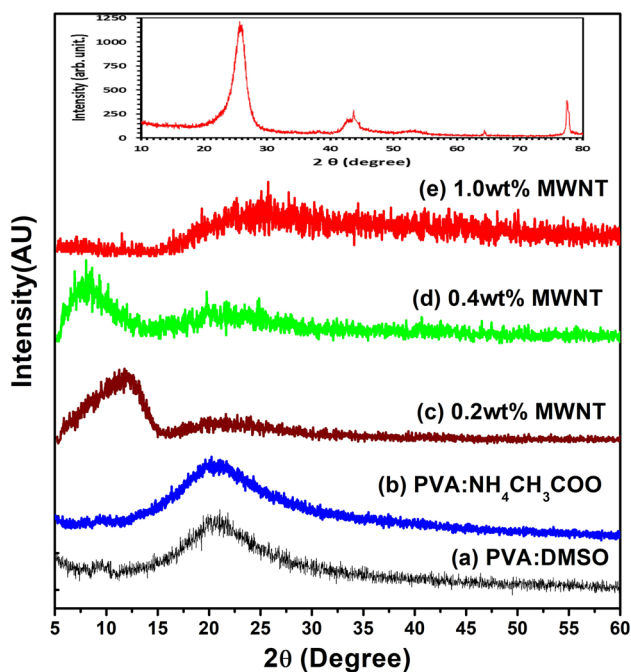


Fig. 1 XRD plot for (PVA-NH₄CH₃COO: \times wt.% MWNT) NCPE system with MWNT concentration: (a) PVA:DMSO, (b) PVA:NH₄CH₃COO, (c) 0.2 wt.%, (d) 0.4 wt.%, and (e) 1.0 wt.%; inset diffractogram representing the XRD peaks of pure MWNTs.

This result indicates that MWNTs are well graphitized. No carbonaceous impurities or metal particles were observed in the MWNTs from the XRD pattern. Crystal planes reflected a pure crystalline structure. Comparison of these XRD data with JCPDS (Card No. 22-1012) data reveals no characteristic peaks other than for the MWNT.¹⁸

In the diffraction profile of the gel membrane (curve-a) without adding any filler (PVA-NH₄CH₃COO-DMSO), apart from environmental effects, two comparatively strong peaks at 9.56° and 20.23° with combined broadening come into view and correspond to characteristic peaks of the polycrystalline PVA-DMSO complex, and the membrane exhibits the salt (NH₄CH₃COO) in the PVA matrix.⁵ A broad peak at $2\theta = 12.1^\circ$ appears in the PVA-NH₄CH₃COO:0.2wt.% MWNT (profile c). This widened peak might be associated with the PVA-NH₄CH₃COO-MWNT interaction, and appears on account of the interaction of the electrolyte with MWNTs, leading to the formation of a nanocomposite which does not match any of the pristine materials: PVA, MWNTs, and NH₄CH₃COO. A further increase in the d value for all the major peaks and the shifting of the peak towards a lower 2θ value with broadening, indicating improvement in the morphology of the PVA-NH₄CH₃COO complex upon incorporation of the MWNT contents. Further, this broadened peak shifts towards lower 2θ values (pattern d) and finally diminishes on the increase of MWNT content up to 1 wt.% in the NCPE gel membrane (pattern e), which reflects

Table I Average crystallite size, degree of crystallinity, and activation energy of nanocomposite polymer gel electrolyte (PVA-NH₄CH₃COO: \times wt.% MWNT) system

Concentration of MWNT contents wt. %	Average crystallites size (nm)	Degree of crystallinity χ_c (%)	Activation energy E_a (eV)
0.0	~ 136	66.2	0.081
0.2	~ 76	59	0.069
0.4	~ 43	32	0.057
1.0	~ 41	31	0.054

complete absorption of the MWNT particles in the PVA matrix/enhanced intercalation of dispersoids in the matrix electrolyte. This again possibly results from physical interaction between constituents (polymer and salt) in the incorporation of the MWNT filler.¹⁶

The average particle size of the gel membrane was found to be 41.48 nm, which is derived from the full width at half-maximum of a more intense peak located at around 20° using Scherrer's formula (Table I), while the degree of crystallinity (χ_c) of the gel membranes with respect to the MWNTs was estimated in order to ascertain improvements in the amorphous nature^{16,17} presuming MWNT to be fully crystalline (Table I), and it can be seen that it decreases with the increase in filler concentration, which again identifies changes in the system morphology on the addition of a filler.

Thermal Studies

Figure 2a–d shows the DSC thermograms characterizing the thermal examination for the (PVA-NH₄CH₃COO:MWNT) system for different MWNT concentrations. Various thermal transitions seen in the DSC patterns for NCPE gel membranes under study are shown in Table II. The shift in the glass transition temperature and melting temperature with composition (Table II) can be related to the flexibility of the polymeric backbone, which in turn affects the conductivity behavior.^{5,19,20}

Deep examination of the DSC scans did not expose any major thermodynamics transition in the range 191–248°C related to the melting transition of the PVA of a system which reveals complete interaction of the polymer constituents with salt (NH₄CH₃COO) leading to the development of new materials with enhanced thermal stability. This can be seen from the DSC scanning of the nanocomposite polymer electrolyte gel membranes which follow a broad endothermic transition in the temperature range 88–146°C. The broadness in the transition can be linked to evaporation of water formed during the interaction of PVA with DMSO, the existence of the melting transition of ammonium acetate salt (99–122°C), and the presence of gel formation.^{5,15} It can be further observed in the thermogram of the gel membrane

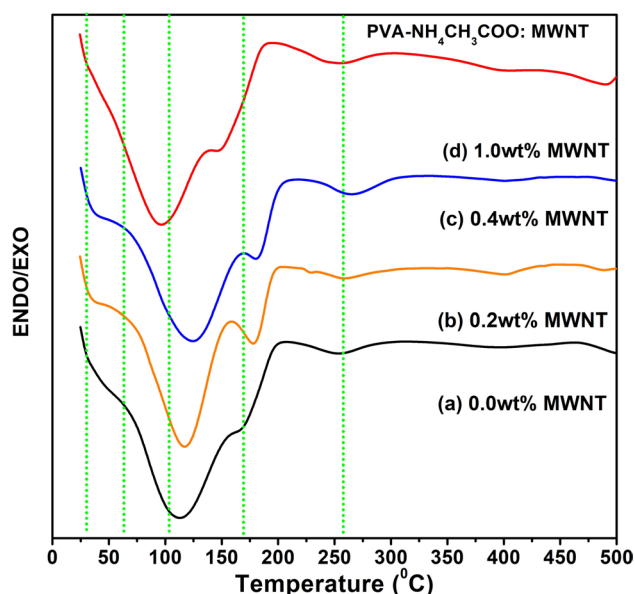


Fig. 2 DSC thermograms of the (PVA-NH₄CH₃COO: × wt.% MWNT) system with: (a) 0.0 wt.%, (b) 0.2 wt.%, (c) 0.4 wt.%, and (d) 1.0 wt.% MWNT-doped NCPE membranes.

Table II. Temperature (°C) peaks of transition in DSC thermograms of the (PVA-NH₄CH₃COO: × wt.% MWNT) system in NCPE membranes

(PVA-NH ₄ CH ₃ COO: × wt.% MWNT)					
wt.% MWNT	<i>P</i> ₁	<i>P</i> ₁	<i>P</i> ₃	<i>P</i> ₄	<i>P</i> ₅
0.0	29	64	112	168	255
0.2	34	67	116	177	259
0.4	36	72	125	181	266
1.0	30	–	98	–	252

that a broad shoulder transition related to the interaction of the polymer-salt or polymer-filler appears in the temperature range (151–198°C). The broadness of this transition increases and the melting temperature of the polymer electrolyte is observed (around 170°C) to shift towards a lower temperature upon the addition of MWNT (scans b–d). This is probably due to an improved interaction between the polymer components in the presence of added salt and filler. Close inspection of the DSC sketch (scan a) shows an endothermic transition in the temperature region around 64°C, which is known as the glass transition of PVA (around 87°C), which shifts towards a lower temperature due to the interaction of PVA between the salt and the polymer.^{5,21,22} Interestingly, all the peaks (Table II) shifted towards lower bands and finally merged in a broad peak on the addition of MWNTs. No transition peak has been seen in the DSC thermogram of pure MWNT (temperature range up to 500°C), as was reported by Han et al.²³ This study confirms that

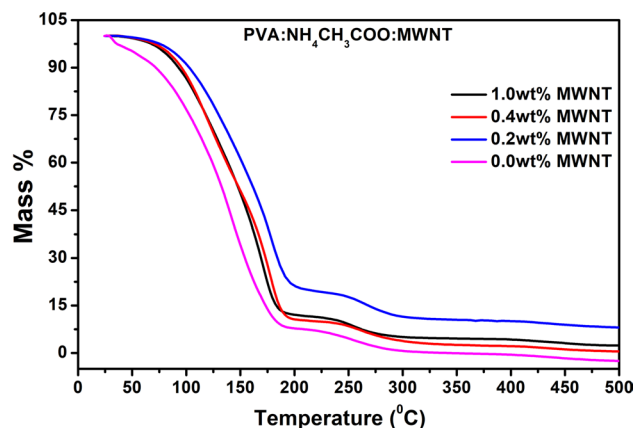


Fig. 3 TGA thermograms of the (PVA-NH₄CH₃COO: × wt.% MWNT) system for different filler concentrations of MWNTs.

MWNTs are the most significant candidate for the enhancement of the thermal stability of the system. Similarly, the broad peak of the third endothermic transition at 245–285°C reaffirms the improvement in thermal stability of composite systems with the existence of the amorphous nature on addition of MWNTs.¹⁹

Figure 3 depicts the TGA thermograms of the nanocomposite polymer gel electrolyte (PVA-NH₄CH₃COO: × wt.% MWNT) system for different MWNT concentrations which represent three major weight losses and corresponding temperature regions which are listed in Table III.

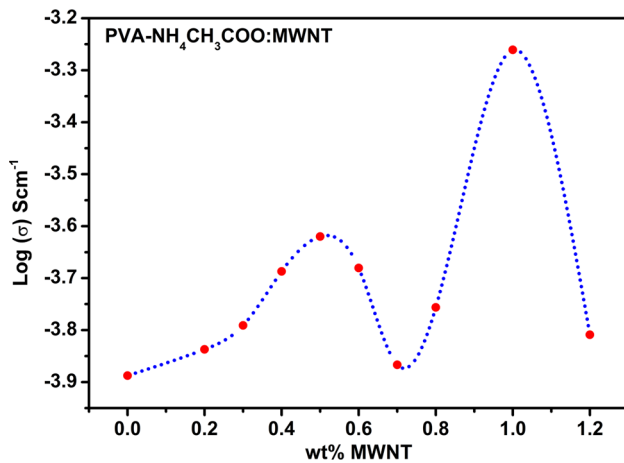
The continuous decrease with the increase in the MWNT nanofiller in the second weight loss temperature range (80–195°C) is attributed to the evaporation of soaked water or the rearrangement of intra- and intermolecular hydrogen-bonded partially order texture.¹⁵ The decrease in loss appears to result from the improved interaction of salt and polymer, leading to improved thermal stability. The TGA thermogram in the temperature range (178–295°C) is correlated to the weight loss values which are quite low and related to decomposition of uncomplexed PVA in the system, which thus also decreases with increases of the MWNTs.

Electrical Conductivity Studies

Figure 4 indicates the role of MWNT concentration on the dc conductivity behavior of NCPE gel electrolytes. Closer examination of the conductivity behavior shows two maxima, one around 0.5 wt.% and the other around 1 wt.% filler concentration, a feature typical of polymer nanocomposite gel electrolytes.¹⁶ A flattening in the conductivity response is noticed beyond 1 wt.% MWNT contents. This can be associated with the fact that all the salt has been dissociated and so charge carrier concentration is limited. It is only the change in system morphology that tends to affect the conductivity, and thus again an enhancement of small

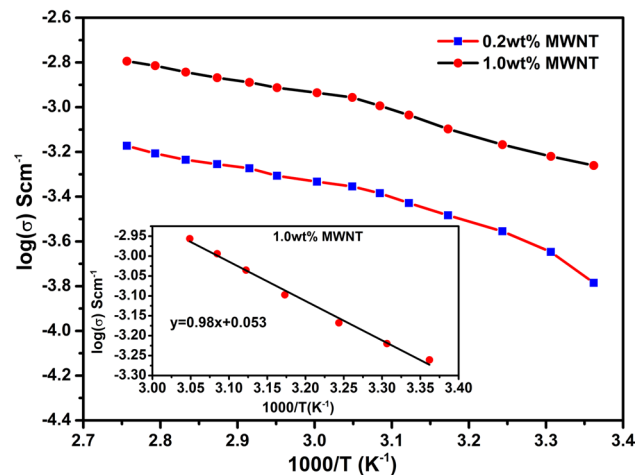
Table III TGA data of the (PVA-NH₄CH₃COO: × wt.% MWNT) system in NCPE membranes

wt.% MWNT	Region-I		Region-II		Region-III	
	T ₁ (°C)	M*% ^a	T ₂ (°C)	M*% ^a	T ₃ (°C)	M*% ^a
0.0	25–75	3.48	75–180	75.53	180–300	14.35
0.2	25–75	3.21	75–195	75.52	195–300	17.37
0.4	25–75	2.70	75–190	68.44	190–300	17.83
1.0	25–80	11.07	80–200	78.43	200–300	10.0

**Fig. 4** Variation of conductivity of nanocomposite polymer electrolyte gel membranes with MWNT filler concentration at room temperature.

magnitude is visible. Another explanation for the rise in conductivity can be provided in terms of the Tsagaropoulos model which was reported earlier.¹⁷ An optimum in conductivity was found at $5.49 \times 10^{-4} \text{ S cm}^{-1}$ for 1wt.% of MWNTs.

The temperature dependence of the electrical conductivity of the polymer gel electrolyte and its composite membranes is presented in Fig. 5. The increase in conductivity with temperature is attributed to a hopping mechanism between coordinated sites, local structural relaxation, and segmental motion of the polymer. The linear region in the low-temperature zone (25–40°C), conductivity obeys an Arrhenius nature as described earlier. This is possibly due to the presence of liquid electrolyte encapsulated by the polymer matrix, i.e., the effect of temperature on conductivity of liquid electrolytes. The mid-temperature regime (40–85°C) conductivity response can be well described by the VTF relationship. When the temperature approaches the glass transition of the complex/pure PVA, the matrix becomes flexible, giving rise to VTF-type behavior. Therefore, all the curves display similar behavior, i.e., a combination of Arrhenius and VTF characteristics.

**Fig. 5** The temperature dependence of the electrical conductivity of the nanocomposite polymer electrolyte gel membranes on the addition of 0.2 and 1 wt.% concentrations of MWNTs; inset conductivity plot of 1wt.% MWNT-filled NCPE with using linear curve fitting in the Arrhenius region for activation energy calculations.

Moreover, the activation energy and other parameters are described by the following Arrhenius relationship:

$$\sigma = \sigma_0 T^{-1} \exp\left(-\frac{E_a}{kT}\right) \quad (6)$$

where, σ_0 is the pre-exponential factor of conductivity and E_a is the activation energy.

On solving this equation, we can find an easy calculation as:

$$\text{Thus, } E_a = 0.08625 \times \text{slope (eV)} \quad (7)$$

Subsequently, the value of the slope is easily found by applying linear curve fitting in the Arrhenius region only, as shown in inset of Fig. 5.

The variation of electrical conductivity for different variations of MWNT-doped polymer gel electrolyte with frequency is shown in Fig. 6. The ac conductivity is evaluated from dielectric data in accordance with Eq. 5. It is apparent from the figure that the ac conductivity increases with frequency in the low-frequency regime followed by a nearly

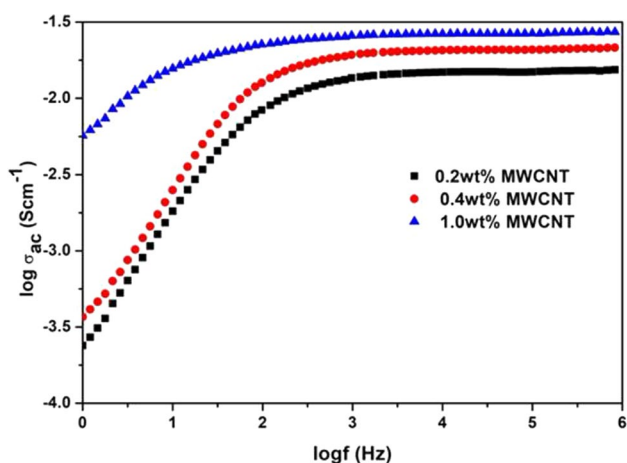


Fig. 6 Variation of ac conductivity with frequency for nanocomposite polymer electrolyte gel membranes containing (■) 0.2 wt.%, (●) 0.4 wt.%, and (▲) 1.0 wt.% MWNT contents.

frequency-independent behavior in the high-frequency regime. The increasing conductivity behavior is connected to the electrode–electrolyte phenomena, i.e., it results from electrode polarization effects. This kind of behavior has been reported for a wide range of nanocomposite polymer electrolytes and also for the (PVA-NH₄SCN:MWNT) electrolytes.¹⁶ It is observed that the increase in filler content enhances ac conductivity. This behavior of ac conductivity can be analyzed by Jonscher's universal power law¹⁷ expressed as:

$$\sigma_{ac} = \sigma_{dc} + A\omega^p \quad (8)$$

where σ_{dc} is the dc conductivity, the value of which can be extracted by extrapolating the plateau region to zero frequency, and maximum observed value is 5.49E-4 S cm⁻¹ for the 1 wt.% MWNT-doped system. Likewise, p can be obtained from the slope of the curve. The value of p is found to vary with filler concentration that the electrical conduction in our system is predominantly due to mobile ionic species. The values of exponent p lie in between 1.0 and 0.5, indicating an ideal long-range pathway and a diffusion-limited hopping process for charge transport in the present electrolyte system. A is pre-exponential factor. The observed frequency dispersion for different composites can also be rationalized with the help of a jump relaxation model,²⁴ since the dynamical effect of the polymer host caused by segmental renewal rates is less significant below microwave frequencies. According to this model, an ion can successfully hop from a site to a neighboring vacant site to contribute to the conductivity. At high frequencies, the probability for ions to hop back increases due to the short time periods. This forward–backward hopping at high frequencies together with relaxation of the dynamic cage potential seems to be responsible for the high-frequency plateau. Activation energy at

room temperature is also reducing slightly on increasing the concentration of MWNTs (Table I). Such low values are normally seen for gel polymer electrolyte systems.²¹ Lowering of activation energy to 1 wt.% MWNT content reaffirms the improvement in electrical conductivity in the presence of nanosized fillers in gel polymer electrolytes.

Dielectric Studies

Variation of dielectric permittivity (ϵ') and dielectric loss (ϵ'') for the different membranes of the NCPE system investigated as a function of frequency at room temperature are shown in Fig. 7a and b using Eqs. 2, 3, and 4. Figure 7a shows strong frequency dispersion of permittivity in the low-frequency region followed by saturation-like behavior. This behavior is due to the fact that, at low frequencies, the dipoles or ionic charges have sufficient time to align with the field before it changes its direction, and consequently the dielectric permittivity is high, whereas the decrease in permittivity value with increasing frequency is attributed to insufficient time for the dipoles to align before the field changes direction²⁵ i.e., the inability of the dipoles to rotate rapidly leads to a lag between the frequency of the oscillating dipoles and the applied field. Upon increasing the MWNT content in the NCPEs, the saturation point shifts towards a higher frequency, possibly due to the decrease in the flexibility of the NCPE system in the presence of added filler. This type of behavior indicates that initially the filler provides almost constant crystalline domain channels up to 1 wt.% filler, and thereafter it starts segregating due to non-complexation in the PVA-NH₄CH₃COO matrix, generating uncomplexed dipolar domains in the matrix. High values of dielectric loss (ϵ'') in the low-frequency regime (Fig. 7b) reflects the reorientation process of the dipoles in polymer chains, which give rise to relaxation peaks in the dielectric loss spectra. The appearance of a broad peak in the frequency range 10 Hz–1 kHz is attributed to the relaxation phenomenon of polymer chain segments.²⁶ Continuous fall in ϵ'' values with increasing filler concentration results from attachment of the filler with the PVA chain through strong interaction between constituents, thereby causing transient cross-links. These cross-links inhibit the relaxation of the dipoles even at low frequencies, which paves the way for decreases in dielectric loss values. Figure 8 shows the plot of $\tan\delta$ versus frequency of NCPE membranes for different filler concentrations at room temperature. The dielectric loss tangent is basically the ratio of the real and imaginary parts of dielectric permittivity discussed earlier.¹² In Fig. 8, the change of slope is observed in the 3–5 kHz frequency range. Essentially, such a change corresponds to the occurrence of a broad peak with the system optimizing the presence of a scaling dipole and is related to the PVA. The maxima of $\tan\delta$ shifted towards a higher frequency and the height of the

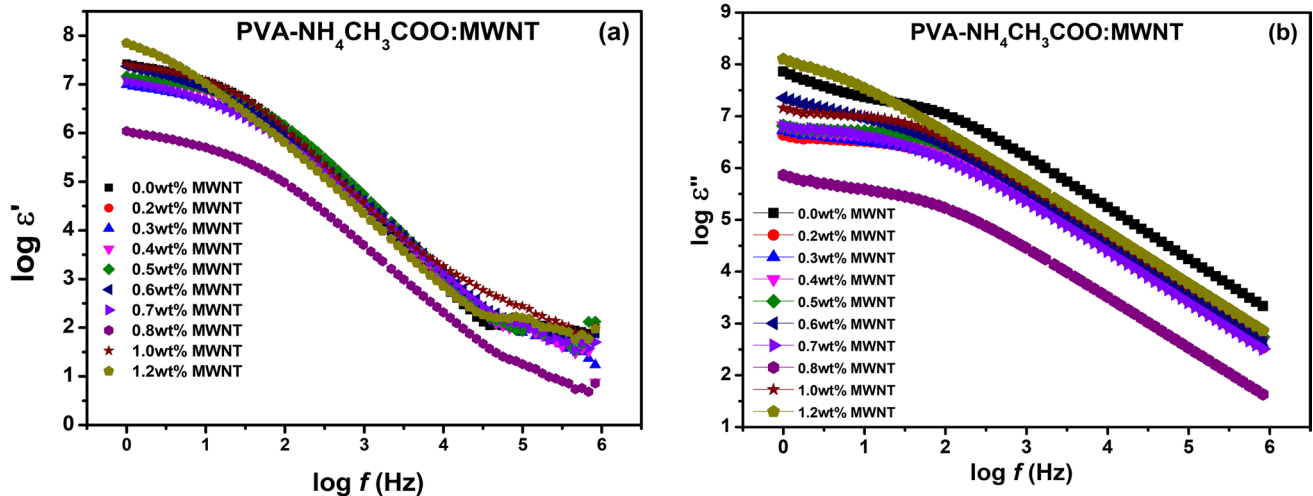


Fig. 7 Variation of (a) dielectric permittivity (ϵ') and (b) dielectric loss (ϵ'') with frequency for the (PVA-NH₄CH₃COO: \times wt.% MWNT) NCPEs at room temperature.

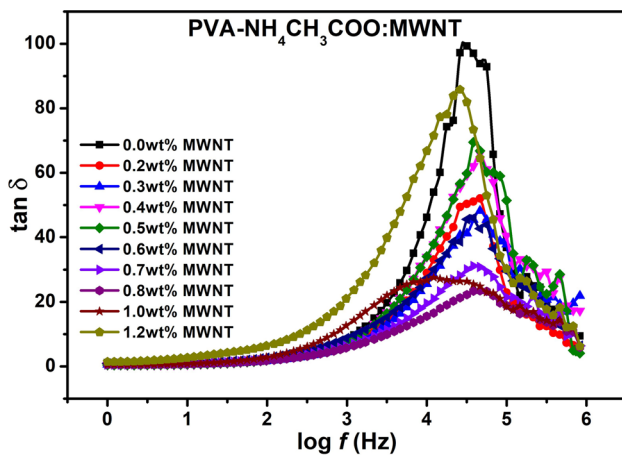


Fig. 8 Variation of $\tan \delta$ versus frequency of NCPE gel membranes for different filler concentrations of MWNT for the (PVA-NH₄CH₃COO: \times wt.% MWNT) system at room temperature.

peak increased with increasing filler content. This is due to the increment in the number of charge carriers for conduction which decreases the resistivity of the samples.²⁷ The relaxation frequency is found to shift towards higher values with the increase in the filler concentration. Increase of the filler content tends to loosen the segmental packing of the PVA polymer chain. Higher values of tangent loss can be attributed to the coupling of ion diffusion with segmental motion of the polymer chain of gel electrolyte membranes. Such a behavior can be successfully explained in terms of a dielectric relaxation process associated with the presence of heterogeneities in the gel matrix. The loss tangent peaks appearing in the plot for the gel membranes infer that the H⁺ ion in the sample was more capable in following the change

in the direction of the applied electric field.²⁸ The results reaffirm that the system is one of the best ion-conducting systems.

Modulus Studies

A further analysis of electric behavior would be more successfully achieved by dielectric modulus (M' and M''), which inhibited the effect of electrode polarization to give a clear indication of the electrical property of the polymer electrolyte. The dielectric modulus was analyzed using the pattern of the frequency of M' and M'' for the (PVA-NH₄CH₃COO:MWNT) NCPE gel membranes for different nanofiller concentrations, as shown in Figs. 9 and 10, respectively. The plots show features of ionic conduction and S-shaped dispersion in M' and a peak in M'' in the higher-frequency range.^{24,29} In modulus formalisms Eqs. 2 and 3, the electrode polarization effect seems to show the possible presence of peaks in the modulus formalism at higher frequencies for all the gel polymer systems, indicating that the gel polymer electrolyte membranes are ionic conductors. Both M' and M'' approached zero at low frequency and show an increase at higher frequency without a relaxation peak. The plots exhibited low values at lower frequencies which might be due to the value of capacitance associated with the electrodes. This further confirmed the non-Debye behavior in the samples. We have also examined the scaling behavior of the modulus function. M' and M'' spectra scaled by M'_{\max} , M''_{\max} scaled by the relaxation frequency f_{\max} are shown in Fig. 11 for different filler concentrations.³⁰ The normalized behavior of the modulus shows that interfacial polarization completely vanishes above 2 kHz frequency. The peak in normalized M'' can be related to translation ion dynamics, and represents the conductivity relaxation of the mobile ions.

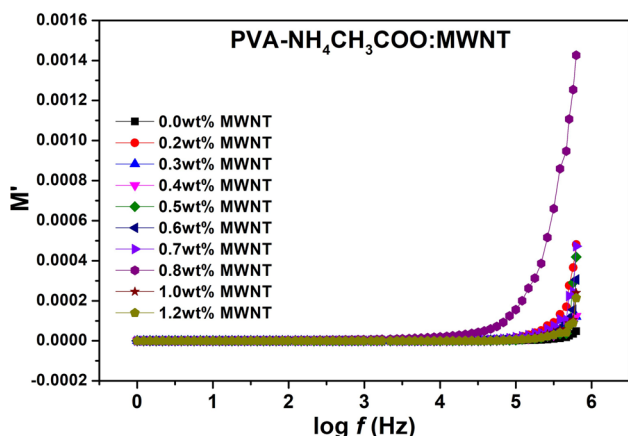


Fig. 9 Variation of the real part of the complex modulus (M') as a function of frequency for the (PVA- $\text{NH}_4\text{CH}_3\text{COO}$: \times wt.% MWNT) system for different MWNT filler concentrations at room temperature.

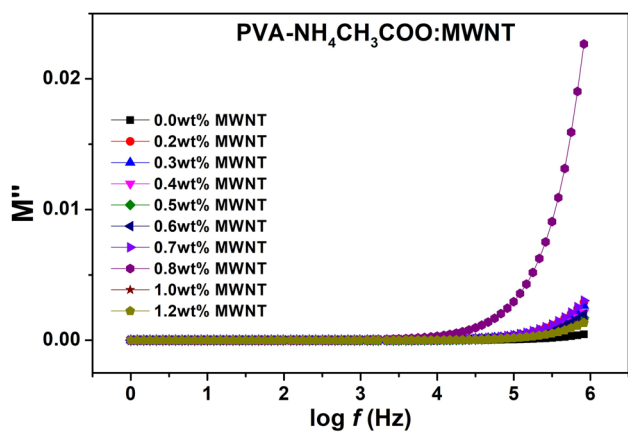


Fig. 10 Variation of the imaginary parts of the complex modulus (M'') as a function of frequency for the (PVA- $\text{NH}_4\text{CH}_3\text{COO}$: \times wt.% MWNT) system for different MWNT filler concentrations at room temperature.

The filler concentration values of M'_{\max} and M''_{\max} decrease and conductivity increases. This behavior is shown in Fig. 12, indicating that the relaxation dynamics vary smoothly with MWNT concentration which promotes improvements in the stability of the system.

Conclusions

The purpose of this investigation was to explore the performance of MWNT filler on the XRD, DSC, and electrical properties of the PVA: $\text{NH}_4\text{CH}_3\text{COO}$:DMSO system. XRD studies reveal the complexation between polymer and salt, and the amorphicity has also improved by admixing

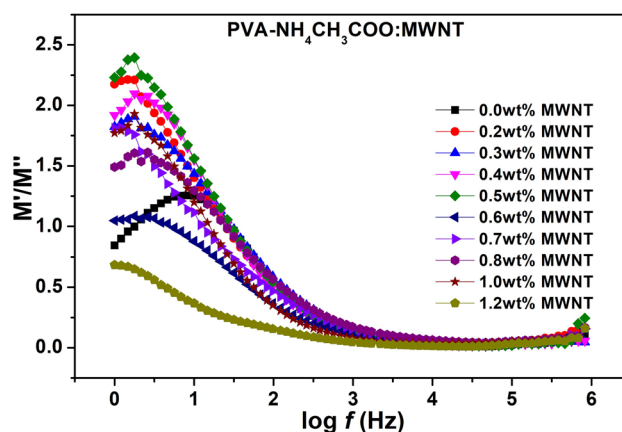


Fig. 11 Variation of M'/M'' as a function of frequency for the (PVA- $\text{NH}_4\text{CH}_3\text{COO}$: \times wt.% MWNT) system for different MWNT filler concentrations at room temperature.

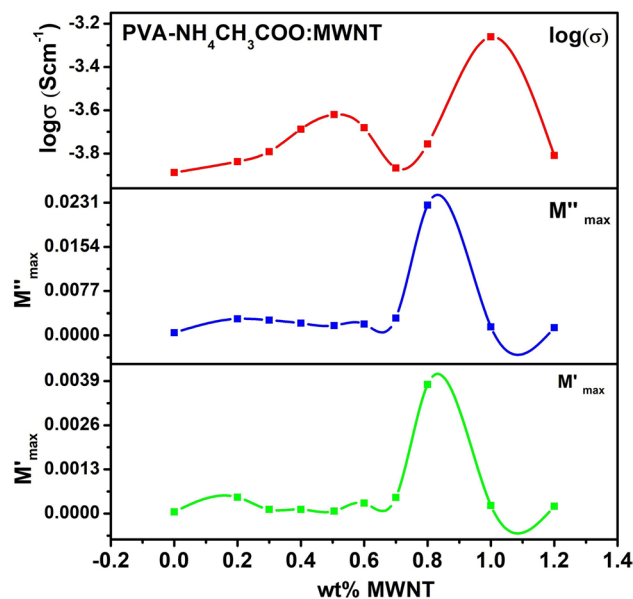


Fig. 12 Variation of M'_{\max} , M''_{\max} , and conductivity with different wt.% MWNT for the (PVA- $\text{NH}_4\text{CH}_3\text{COO}$: \times wt.% MWNT) system.

nanosized MWNTs. DSC studies show improvement in thermal behavior of the system subsequent to nanotube addition. The dc conductivity has been found to increase and obey two conductivity maximas with increasing MWNT content, and reached optimum at 1 wt.% MWNT-filled nanocomposite electrolyte. A temperature-dependent study of dc conductivity response is described by the combination of Arrhenius and VTF behaviors. The ac conductivity responses in all the cases are well described by a jump relaxation model and the Jonscher power law. The highest ac conductivity values are possibly due to the creation of extra hopping sites assisting the ion hopping. The present investigations recommend nanotube-embedded

NCPE gel membranes as a suitable system for achieving electrochemically and thermally stable electrolytes with an appropriate environmentally friendly H⁺ ion (proton) conducting-based system. The electrical conductivity is improved and exhibits good electrode–electrolyte contact. Such properties are expected to open up application areas, particularly in supercapacitors.

Acknowledgments Authors are grateful to the Department of Physics, APS University for providing Electrochemical Analyzer for experimental analysis of conductivity (dielectric & modulus studies). Authors are also thankful to Department of Physics, Pt. Ravishankar Shukla University, Raipur (CG) for providing XRD analysis and Department of Physics, Central University Sagar (M.P.) for DSC analysis.

Funding This research did not receive any specific grant from funding agencies like public, commercial, or not for profit sectors.

Conflict of interest The authors declare that there is no conflict of interest regarding the publication of this article.

References

- M.S. Al Ja'farawy, D.N. Hikmah, U. Riyadi, A. Purwanto, and H. Widiyandari, A review: the development of SiO₂/C anode materials for lithium-ion batteries. *J. Electron. Mater.* 50, 6667 (2021).
- S. Pathania, J.J.L. Hmar, B. Verma, T. Majumder, V. Kumar, and P. Chinnamuthu, Titanium dioxide (TiO₂) sensitized zinc oxide (ZnO)/conducting polymer nanocomposites for improving performance of hybrid flexible solar cells. *J. Electron. Mater.* 51, 5986 (2022).
- H.D. Wu, I.D. Wu, and F.C. Chang, The interaction behavior of polymer electrolytes composed of poly(vinyl pyrrolidone) and lithium perchlorate (LiClO₄). *Polymer* 42, 555 (2001).
- K. Mishra, S.A. Hashmi, and D.K. Rai, Nanocomposite blend gel polymer electrolyte for proton battery application. *J. Solid State Electrochem.* 17, 785 (2013).
- A. Awadhia and S.L. Agrawal, Structural, thermal and electrical characterizations of PVA:DMSO:NH₄SCN gel electrolytes. *Solid State Ionics* 178, 951 (2007).
- A.M. Stephen, Review on gel polymer electrolytes for lithium batteries. *Eur. Polym. J.* 42, 21 (2006).
- C. Cazan, A. Enesca, and L. Andronic, Synergic effect of TiO₂ filler on the mechanical properties of polymer nanocomposites. *Polymers* 13, 2017 (2021).
- S. Choudhary and R.J. Sengwa, Effects of different inorganic nanoparticles on the structural, dielectric and ion transportation properties of polymers blend based nanocomposite solid polymer electrolytes. *Electrochim. Acta* 247, 924 (2011).
- C.P. Singh, P.K. Shukla, and S.L. Agrawal, Ion transport studies in PVA:NH₄CH₃COO gel polymer electrolytes. *High Perform. Polym.* 32, 208 (2020).
- T.V. Rajendran and V. Jaisankar, Preparation, characterisation and conductivity studies of supramolecular polymer/ferrite nanocomposites. *Mater. Today Proc.* 2, 4421 (2015).
- A.P. Khandale, S.S. Bhoga, and S.K. Gedam, Study on ammonium acetate salt-added polyvinyl alcohol-based solid proton-conducting polymer electrolytes. *Ionics* 19, 1619 (2013).
- L. Ranjta, C.P. Singh, and N. Rai, Experimental investigations on nano-ferrite embedded nanocomposite polymer electrolytes for proton-conducting rechargeable batteries application. *Mater. Today Proc.* 54, 702 (2022).
- G.R. Baymuratova, A.V. Chernyak, A.A. Slesarenko, G.Z. Tuli-baeva, V.I. Volkov, and O.V. Yarmolenko, Specific features of ion transport in new nanocomposite gel electrolytes based on cross-linked polymers and silica nanoparticles. *Russ. J. Electrochem.* 55, 529 (2019).
- S. Manzetti and J.C.P. Gabriel, Methods for dispersing carbon nanotubes for nanotechnology applications: liquid nanocrystals, suspensions, polyelectrolytes, colloids and organization control. *Int. Nano Lett.* 9, 31 (2019).
- N. Rai, C.P. Singh, and L. Ranjta, Structural, thermal and electrical studies of Al₂O₃ nanoparticle soaked electrolyte gel films for novel proton conducting (H⁺ ion) eco-friendly device applications. *Am. J. Nano Res. Appl.* 10, 1 (2022).
- S.L. Agrawal and N. Rai, DMA and conductivity studies in PVA:NH₄SCN:DMSO:MWNT nanocomposite polymer dried gel electrolytes. *J. Nanomater.* 435625, 1 (2015).
- S.L. Agrawal, N. Rai, T.S. Natarajan, and N. Chand, Electrical characterization of PVA-based nanocomposite electrolyte nanofibre mats doped with a multiwalled carbon nanotube. *Ionics* 19, 145 (2013).
- M. Farbod, S.K. Tadavani, and A. Kiasat, Surface oxidation and effect of electric field on dispersion and colloids stability of multiwalled carbon nanotubes. *Colloids Surf. A Physicochem. Eng. Asp.* 384, 685 (2011).
- N. Chand, N. Rai, T.S. Natarajan, and S.L. Agrawal, Fabrication and characterization of nano Al₂O₃ filled PVA:NH₄SCN electrolyte nanofibers by electrospinning. *Fibers Polym.* 12, 438 (2011).
- S.L. Agrawal and A. Awadhia, DSC and conductivity studies on PVA based proton conducting gel electrolytes. *Bull. Mater. Sci.* 27, 523 (2004).
- N. Chand, N. Rai, S.L. Agrawal, and S.K. Patel, Morphology, thermal, electrical and electrochemical stability of nanoaluminum-oxide-filled polyvinyl alcohol composite gel electrolyte. *Bull. Mater. Sci.* 34, 1297 (2011).
- S.L. Agrawal, N. Rai, and N. Chand, Dynamic mechanical, DSC, and electrical investigations on nano Al₂O₃ filled PVA:NH₄SCN:DMSO polymer composite dried gel electrolytes. *Int. J. Polym. Mater.* 62, 61 (2013).
- W. Han, W. Song, Y. Shen, C. Ge, R. Zhang, and X. Zhang, Multiwalled carbon nanotubes encapsulated polystyrene: a facile one-step synthesis, electrical and thermal properties. *J. Mater. Sci.* 54, 6227 (2019).
- K. Funke, Jump relaxation in solid electrolytes. *Prog. Solid State Chem.* 22, 111 (1993).
- M.H. Buraidah, L.P. Teo, S.R. Majid, and A.K. Arof, Ionic conductivity by correlated barrier hopping in NH₄I doped chitosan solid electrolyte. *Physica* 404, 1373 (2009).
- R. Leones, M. Fernandes, F. Sentaninc, I. Cesarino, J.F. Lima, V. Bermudez, A. Pawlicka, C.J. Magond, J.P. Donoso, and M.M. Silva, Ionically conducting Er³⁺-doped DNA-based bio membranes for electrochromic devices. *Electrochim. Acta* 120, 327 (2014).
- S.R. Majid and A.K. Arof, Electrical behaviour of proton-conducting chitosan-phosphoric acid-based electrolyte. *Physica* 390, 209 (2007).
- C.S. Ramya, S.S. Ekarapandian, G. Hirankumar, T. Savita, and P.C. Angelo, Investigation on dielectric relaxation of PVP-NH₄SCN polymer electrolyte. *J. Non-Cryst. Solids* 354, 1494 (2008).
- S.L. Agrawal, M. Singh, N. Asthana, M.M. Dwivedi, and K. Pandey, Dielectric and ion transport studies in (PVA:LiC₂H₃O₂:Li₂Fe₃O₈) polymer nanocomposite electrolyte. *Int. J. Polym. Mater.* 60, 276 (2011).
- S.L. Agrawal, M. Singh, N. Asthana, M.M. Dwivedi, and K. Pandey, Dielectric relaxation studies on [PEO-SiO₂]:NH₄SCN

nanocomposite polymer electrolyte films. *J. Mater Sci.* 44, 6060 (2009).

Publisher's Note Springer Nature remains neutral with regard to jurisdictional claims in published maps and institutional affiliations.

Springer Nature or its licensor (e.g. a society or other partner) holds exclusive rights to this article under a publishing agreement with the author(s) or other rightsholder(s); author self-archiving of the accepted manuscript version of this article is solely governed by the terms of such publishing agreement and applicable law.